Journal of Translational Medicine

RESEARCH

Open Access

LIN28A-dependent lncRNA NEAT1 aggravates sepsis-induced acute respiratory distress syndrome through destabilizing ACE2 mRNA by RNA methylation

Jun Liu[1†], Xiang Li[1†], Peng Yang[2†], Yufeng He[3], Weilong Hong[4], Yawei Feng[1*] and Zhiqiang Ye[4*]

Abstract

Background Acute respiratory distress syndrome (ARDS) is a life-threatening and heterogeneous disorder leading to lung injury. To date, effective therapies for ARDS remain limited. Sepsis is a frequent inducer of ARDS. However, the precise mechanisms underlying sepsis-induced ARDS remain unclear.

Methods Here RNA methylation was detected by methylated RNA immunoprecipitation (MeRIP), RNA stability was determined by RNA decay assay while RNA antisense purification (RAP) was used to identify RNA-protein interaction. Besides, co-immunoprecipitation (Co-IP) was utilized to detect protein-protein interaction. Moreover, mice were injected with lipopolysaccharide (LPS) to establish sepsis-induced ARDS model in vivo.

Results This study revealed that long non-coding RNA (lncRNA) nuclear-enriched abundant transcript 1 (NEAT1) aggravated lung injury through suppressing angiotensin-converting enzyme 2 (ACE2) in sepsis-induced ARDS models in vitro and in vivo. Mechanistically, NEAT1 declined *ACE2* mRNA stability through heterogeneous nuclear ribonucleoprotein A2/B1 (hnRNPA2B1) in lipopolysaccharide (LPS)-treated alveolar type II epithelial cells (AT-II cells). Besides, NEAT1 destabilized *ACE2* mRNA depending on RNA methylation by forming methylated NEAT1/hnRNPA2B1/*ACE2* mRNA complex in LPS-treated AT-II cells. Moreover, lin-28 homolog A (LIN28A) improved NEAT1 stability whereas insulin-like growth factor 2 mRNA binding protein 3 (IGF2BP3) augmented NEAT1 destabilization by associating with LIN28A to disrupt the combination of LIN28A and NEAT1 in LPS-treated AT-II cells. Nevertheless, hnRNPA2B1 increased NEAT1 stability by blocking the interaction between LIN28A and IGF2BP3 in LPS-treated AT-II cells.

Conclusions These findings uncover mechanisms of sepsis-triggering ARDS and provide promising therapeutic targets for sepsis-induced ARDS.

[†]Jun Liu, Xiang Li and Peng Yang contributed equally to this work.

*Correspondence:
Yawei Feng
fengyaw@mail.sysu.edu.cn
Zhiqiang Ye
yezhiq@mail.sysu.edu.cn

Full list of author information is available at the end of the article

Keywords Acute respiratory distress syndrome, Sepsis, NEAT1, ACE2, RNA methylation, RNA stability

Background

Acute respiratory distress syndrome (ARDS) is a life-threatening and heterogeneous disorder that results in lung injury [1–3]. The clinicopathological correlates of ARDS include severe lung inflammation, depletion of surfactant, increased pulmonary vascular permeability, loss of aerated lung tissue, refractory hypoxemia, reduced lung compliance, and elevation of dead space [2–4]. Despite significant advances in our understanding of the molecular mechanisms inducing ARDS and management of ARDS patients, effective therapies remain limited, and the mortality rate of patients with ARDS is as high as 40% [5].

ARDS can arise from various diseases and pathological conditions, such as coronavirus disease 2019 (COVID-19) and sepsis [6, 7]. Sepsis, a pathological condition resulting from an excessive immune response to pathogen infections, is considered a frequent inducer of ARDS [8, 9]. Several studies have suggested that sepsis can lead to ARDS [10, 11]. However, the underlying mechanisms of sepsis-induced ARDS remain unclear. Therefore, it is urgent to investigate the mechanisms through which sepsis triggers ARDS and explore novel therapeutic targets for sepsis-induced ARDS.

Numerous studies have indicated that severe acute respiratory syndrome coronavirus 2 (SARS-CoV-2) associated with COVID-19 enters host cells through the receptor angiotensin-converting enzyme 2 (ACE2) inducing lung injury in vivo and in vitro [12, 13]. Additionally, host cells can protect from ARDS by reducing angiotensin II (Ang II) expression by inactivating renin–angiotensin system (RAS) after infection with the SARS coronavirus [14]. Therefore, ACE2 is downregulated in the lungs of SARS coronavirus-infected mice with ARDS [14, 15]. Although ACE2 expression is also decreased in the lungs of mice with ARDS induced by sepsis [12], the role of ACE2 in sepsis-induced ARDS remains largely unknown.

A previous study has indicated that the long non-coding RNA (lncRNA) nuclear-enriched abundant transcript 1 (NEAT1) associates with ACE2 expression in SARS-CoV-2-infected lung cells [16]. Growing evidence suggests that NEAT1 contributes to sepsis-induced ARDS. For instance, the NEAT1 level is increased in the plasma of patients with sepsis-induced ARDS, and a higher NEAT1 level is associated with an increased risk of ARDS and higher mortality in sepsis patients [17]. Mechanistically, NEAT1 exacerbates sepsis-induced ARDS by targeting microRNA (miRNA) miR-27a, leading to the upregulation of phosphatase and tensin homolog (PTEN) expression [18]. Furthermore, NEAT1 might aggravate sepsis-induced ARDS by suppressing high-mobility group box1 (HMGB1)-receptors for the advanced glycation end products (RAGE) pathway [19]. Nevertheless, the regulatory effect of NEAT1 on ACE2 in sepsis-induced ARDS remains unclear.

RNA methylation plays a crucial role in various diseases by regulating RNA stability, transportation, shearing, and translation, including sepsis [20, 21]. A recent study has revealed that RNA methylation of peripheral blood mononuclear cells (PBMC) is associated with the gut microbiome and serum metabolomic profile of patients with sepsis-associated encephalopathy [22]. Additionally, methylation of suppressor of cytokine signaling 1 (SOCS1) mRNA is essential to suppress macrophage activation in response to sepsis [21]. However, the function of RNA methylation on NEAT1 in sepsis-induced ARDS remains unidentified.

In addition, the RNA-binding protein heterogeneous nuclear ribonucleoprotein A2/B1 (hnRNPA2B1) is crucial for the function of NEAT1. A recent study has demonstrated that NEAT1 reduces the degradation of regulation of nuclear pre-mRNA domain containing 1B (RPRD1B) mRNA through recruiting hnRNPA2B1 in gastric cancer cells [23]. Moreover, as an m6A "reader" protein, hnRNPA2B1 is also involved in the function of methylated lncRNA. For instance, m6A methylated lncRNA RP11 induces the mRNA degradation of E3 ligases through the methylated lncRNA RP11/hnRNPA2B1/ target mRNA complex [24]. Nevertheless, the effect of hnRNPA2B1 on NEAT1 in sepsis-induced ARDS remains unclear.

Therefore, the primary aim of the current study was to investigate whether ACE2 and NEAT1 regulated sepsis-induced ARDS through RNA methylation and hnRNPA2B1.

Materials and methods

Cell culture

AT-II cells, bought from the Cell Bank at the Chinese Academy of Sciences, Shanghai, China, were cultured in Dulbecco's modified Eagle's medium (DMEM, Gibco BRL, Grand Island, NY, USA) supplemented with penicillin (100 units/mL, Gibco BRL) and fetal bovine serum (FBS) (10%, Gibco BRL) at 37 °C in a humidified atmosphere with 5% CO_2.

Cell treatment

To establish an in vitro modal of sepsis-induced ARDS, AT-II cells were treated with 100 ng/mL lipopolysaccharide (LPS) (#S11060, Yuanye, Shanghai, China) for 24 h as previously described [25, 26]. For RNA interference of

Table 1 Sequences of siRNAs

Genes		Sequences (5′-3′)
NEAT1 siRNA	Sense	CCUUUUGGACUUUUCUCUAGG
	Antisense	UAGAGAAAAGUCCAAAAGGAG
HnRNPA2B1 siRNA	Sense	CUGUUUGUUGGCGGAAUUAAA
	Antisense	UAAUUCCGCCAACAAACAGCU
METTL3 siRNA	Sense	GCUGGACUUGGGAUGAUAUUA
	Antisense	GGAATGGTCAGCATAGGTTACA
METTL14 siRNA	Sense	CCGTGGACGAGAAAGAAATAGA
	Antisense	AAAGAAGGTTAGAGGAGGATGAATAG
siRNA NC	Sense	UUCUCCGAACGUGUCACGU
	Antisense	ACGUGACACGUUCGGAGAA

Table 2 Sequences of primers

Genes		Sequences (5′-3′)
NEAT1	Forward	GGCAGGTCTAGTTTGGGCAT
	Reverse	CCTCATCCCTCCCAGTACCA
ACE2	Forward	GGTCTTCTGTCACCCGATTT
	Reverse	CATCCACCTCCACTTCTCTAAC
HnRNPA2B1	Forward	CCAGGACCAGGAAGTAACTTTAG
	Reverse	CCTCCTCTTCCTCCTCCATAA
METTL3	Forward	TGCTGTGTCCATCTGTCTTG
	Reverse	GGAATGGTCAGCATAGGTTACA
METTL14	Forward	CCGTGGACGAGAAAGAAATAGA
	Reverse	AAAGAAGGTTAGAGGAGGATGAATAG
LIN28A	Forward	GTAGGGCTGTGGATTTCTTCTT
	Reverse	AAAGAAGGTTAGAGGAGGATGAATAG
GAPDH	Forward	AACGGATTTGGTCGTATTGGG
	Reverse	CCTGGAAGATGGTGATGGGAT

NEAT1, hnRNPA2B1, methyltransferase 3 (METTL3), METTL14, and lin-28 homolog A (LIN28A), small interfering RNA (siRNA) and non-targeting siRNA (siNC) were synthesized by Hytran Biotech (Guangzhou, Guangdong, China) and transfected into AT-II cells by Lipofectamine 2000 (Thermo Fisher Scientific, Waltham, MA, USA). Table 1 shows sequences of siRNAs.

Quantitative reverse transcription-PCR (qRT-PCR)

Initially, we used a Trizol reagent from Invitrogen (Carlsbad, CA, USA) to isolate total RNA from AT-II cells. Subsequently, the PrimeScript II 1st Strand cDNA Synthesis Kit (Takara, Dalian, Liaoning, China) was utilized to synthesize cDNA from RNA. Following this qRT-qPCR was carried out using a 7500 Fast Real-Time PCR system (Applied Biosystems, Foster City, CA, USA) with SYBR Premix Ex Taq II (Takara). Finally, the relative expression of target genes was normalized to *GAPDH* and the data were given by $2^{-\triangle\triangle Ct}$ relative to the control group. The primers utilized in this study are listed in Table 2.

Western blot (WB)

Proteins from AT-II cells were first isolated by RIPA buffer (Cell Signaling Technology, Danvers, MA, USA). Then proteins were separated by electrophoresis into SDS-polyacrylamide gel followed by the transfer onto the PVDF membrane (Millipore, Bedford, MA, USA). Next, membranes were blocked for 1 h utilizing 5% non-fat milk at room temperature (RT) and then incubated overnight at 4 °C with primary antibodies. The next day membranes were washed with Tris-buffered saline containing 0.1% Tween20 (TBST) and then incubated with secondary antibodies for 1.5 h at RT. After incubation, the Chemiluminescence Detection Kit (#P0018S, Beyotime, Shanghai, China) was used to visualize protein signals. Densitometry of target protein bands was qualified using Image J software. The primary antibodies used in this study for WB included anti-ACE2 (1:1000, #21115-1-AP, Proteintech, Rosemont, IL, USA), anti-hnRNPA2B1 (1:1000, #14813-1-AP, Proteintech), anti-LIN28A (1:1000, #bs-8443R, Bioss, Beijing, China), anti-IGF2BP3 (1:1000, #14642-1-AP, Proteintech) and anti-GAPDH (1:10000, #KC-5G5, Aksomics, Shanghai, China).

Enzyme-linked immunosorbent assay (ELISA)

Levels of IL-1β, IL-18 and TNF-α in cellular supernatant of AT-II cells and mouse serum were measured by ELISA using IL-1β ELISA Kit (#DG10298H, Winter Song Boye Biotechnology, Beijing, China), IL-18 ELISA Kit (#DG10053H, Winter Song Boye Biotechnology) and TNF-α ELISA Kit (#DG10307H, Winter Song Boye Biotechnology) according to the manufacturer's instructions, respectively. Briefly, 10μL sample/well were diluted by 40μL blocking buffer and incubated with 100μL ELISA reagent for 1 h at 37° C. Then plates were washed and incubated with 100μL/well of substrate solution for 15 min at RT in the dark. Next, the reaction was stopped by 25 μL/well of 2 M H_2SO_4 and optical density (OD) at 450 nm.

CCK-8 cell proliferation assay

First, 1×10^4 AT-II cells were collected into 96-well plates followed by the incubation with a volume of 100μL of medium containing 10μL CCK-8 reagent (Beyotime) for 2 h at RT. Next, OD values were detected at an excitation wavelength of 450 nm to assess the cell proliferation rate.

Flowcytometric analysis for cell apoptosis

AT-II cells (3×10^5) were collected and incubated with 100μL phosphate-buffered saline (PBS) supplemented 2 μg/mL AnnexinV (#KGA106, KeyGEN BioTECH, Nanjing, Jiangsu, China) in the dark for 15 min at RT. Then cells were washed twice using PBS and treated with 5μg/mL propidium iodide (PI, #ST511, Beyotime). The apoptosis of AT-II cells was then analyzed by flow cytometry (FACSARIA, BD Biosciences, San Jose, CA, USA) and qualified by FlowJo software.

Lentivirus packaging

To target NEAT1, a specific sequence of shRNA was created based on NEAT1 siRNA. Two single DNA strands of shRNA targeting NEAT1 were produced and cloned into the lentivirus interference vector pLP/VSVG (#K497000, Invitrogen) to develop the lentivirus shRNA interference vector of NEAT1 (shNEAT1). In addition, the open reading frame of the *ACE2* gene was cloned into pLP/VSVG (Invitrogen) to generate a lentivirus expression vector of the *ACE2* gene (ACE2-OE) as previously described [27]. shNEAT1 or ACE2-OE were co-transfected with lentivirus packaging helper plasmids pLP1 and pLP2 (#K497000, Invitrogen) into 293 FT cells. The Lipofectamine 2000 from Invitrogen was used for this packaging. The lentivirus stock solution was collected and concentrated, and the virus titer was determined.

Establishment of ARDS model in vivo

In this study, 25 6-week-old male C57 mice were randomly divided into five groups (5 mice per group), with one group considered as the control group. To establish sepsis-induced ARDS model in vivo, mice were subjected to intraperitoneal injection of 4 mg/kg LPS in 0.9% NaCl [28, 29], while control mice were injected with an equivalent volume of saline. Lentivirus for NEAT1 silence or ACE2 overexpression was delivered by tail-vein injection. Mice were anesthetized with pentobarbital and euthanized using CO_2 at 48 h after LPS injection. All animal experiments were approved by the Animal Ethics Committee of Sun Yat-sen University (#SYSU-IACUC-2022-000058).

TUNEL assay

After euthanization, mouse lungs were excised, and fixed by 4% paraformaldehyde (PFA) overnight and embedded in paraffin wax. The lung tissues were sectioned (5 μm), and Terminal deoxynucleotidyl transferase-mediated dUTPnick-end labeling (TUNEL) was applied utilizing TMR (red) Tunel Cell Apoptosis Detection Kit (#G1502, Servicebio, Wuhan, Hubei, China). Lung sections were photographed using an Eclipse Ci-L microscope (Nikon, Tokyo, Japan), and the rate of apoptotic cells in lung tissues was analyzed using Image J.

Hematoxylin and eosin staining

Initially, mice were anesthetized using pentobarbital and then euthanized by CO_2. Next, mouse lung tissues were collected and fixed overnight with 4% PFA and embedded in paraffin wax. Then the mouse lung tissues were sectioned into 5 μm thickness followed by H&E staining using Hematoxylin-Eosin/HE Staining Kit (#G1120, Solarbio Biotechnology, Beijing, China) according to the instructions of manufacturer. After staining, Lung sections were photographed by a microscope (Eclipse Ci-L, Nikon).

Dual-luciferase reporter assay

Transcription start site (TSS) and 2500 bp upstream TSS of human *ACE2* promoter were cloned into luciferase reporter gene plasmid pGL3 to construct reporter gene plasmid containing *ACE2* promoter by Hytran Biotech. AT-II cells were then co-transfected with the reporter gene plasmid containing *ACE2* promoter and siNRAT1 or siCtrl. Following transfection for 48 h, AT-II cells were harvested, and the luciferase activity was identified by the Dual luciferase reporter assay system (Promega, Madison, WI, USA).

RNA decay assays

Actinomycin D at a concentration of 5 μg/mL (#A9415, Sigma-Aldrich, St. Louis, MO, USA) was added into the culture medium of AT-II cells to inhibit DNA transcription. The cells were collected at 0, 1, 2, 3, 4, and 5 h after actinomycin D treatment, and RNA levels were detected by qRT-PCR. Besides, the RNA level at other times was calculated as the fold change from the level identified at 0 h after actinomycin D treatment. Taking the time after actinomycin D treatment as the abscissa and the RNA level as the ordinate, the slope of the decline curve was generated by linear regression. Subsequently, the half-life ($t_{1/2}$) of RNA was calculated based on the relationship of half-life (0.693\slope and the formula was −0.693\slope when the slope is negative). In thish study, GAPDH was the negative control for all RNA decay assays.

RNA antisense purification (RAP)

First, biotin-labeled NEAT1 probes were generated by Hytran Biotech. Then, 1% formaldehyde was utilized (10 min at RT) to crosslink AT-II cells which were subsequently halted by glycine. After lysis of the AT-II cells lysis buffer, DNase was added (10 min/37℃) to get rid of shear DNA. Prior to the incubation with AT-II cell lysis (45℃/ 180 min) in 1×hybridization buffer, both biotin-labeled NEAT1 probes and streptavidin magnetic beads were mixed for 30 min at RT. After incubation, streptavidin beads were isolated via magnetic separation and washed five times with buffer at 35℃. Finally, RNA isolated via immunoprecipitation was eluted and analyzed by qRT-PCR. Simultaneously, WB analysis using hnRNPA2B1 antibody, LIN28A antibody, and IGF2BP3 antibody confirmed protein enrichment after immunoprecipitation.

Methylated RNA immunoprecipitation (MeRIP)

AT-II cells were collected and lysed, followed by the disruption of RNA by ultrasound. Subsequently, cell lysate was incubated with m6A antibody (1:500, #ab208577,

Abcam, Cambridge, MA, USA) at 4℃ overnight. Then m6A antibody and methylated RNA fragments were captured by avidin magnetic beads, and the level of methylated RNA was measured by qRT-PCR.

Co-immunoprecipitation (Co-IP)

AT-II cells were initially disrupted with a non-denaturing lysis buffer from Sigma-Aldrich. Subsequently, approximately 300 μg proteins were incubated with 1 μg IGF2BP3 antibody (#14642-1-AP, Proteintech) and 25μL protein A/G magnetic beads (Thermo Fisher Scientific) for immunoprecipitation overnight at 4℃. After incubation, a magnetic separation device was utilized to collect the beads. The precipitated proteins were then washed with washing buffer 4 times at RT. Finally, proteins binding with IGF2BP3 were detected by WB using anti-LIN28A and anti-hnRNPA2B1. In addition, rabbit IgG was served as a negative control.

Statistical analysis

Quantitative data were presented as mean±standard deviation (SD). SPSS 20 software (SPSS Inc., Chicago, IL, USA) was used for analysis of statistical differences. The comparison between the two groups was analyzed by the unpaired Student's t-test, while the post-hoc Tukey's test following One-way ANOVA was utilized to detect significant results among multiple groups. $P<0.05$ was considered as statistically significant.

Results

NEAT1 aggravates lung injury caused by sepsis-induced ARDS through suppressing ACE2 in vitro and in vivo

To establish the in vitro sepsis-induced ARDS model, AT-II cells were treated with LPS. Next, NEAT1 expression was detected by qRT-PCR. Results showed that the administration of LPS significantly upregulated NEAT1 levels in AT-II cells compared to other cells ($P<0.05$) (Fig. 1A), consistent with previous studies [18, 19]. In contrast, the silence of NEAT1 by siRNA significantly decreased NEAT1 expression ($P<0.05$) (Fig. 1B). Analysis of qRT-PCR and WB revealed that LPS significantly ($P<0.05$) reduced ACE2 mRNA level and protein level (Fig. 1C and D). Besides, the silence of NEAT1 reserved the effect of LPS on ACE2 expression (Fig. 1C and D). These results suggest that NEAT1 suppresses ACE2 expression in sepsis-induced ARDS.

Then the role of ACE2 in sepsis-induced ARDS was explored in vitro. Results showed that LPS significantly increased levels of IL-1β ($P<0.01$), IL-18 ($P<0.0001$), and TNFα ($P<0.001$) in AT-II cells (Fig. 1E). Additionally, LPS significantly inhibited proliferation and induced apoptosis of AT-II cells (Fig. 1F and G). However, both NEAT1 silence and ACE2 overexpression neutralized the effects of LPS on AT-II cells (Fig. 1E, F, and G).

In addition, mice were treated with LPS to construct the in vivo sepsis-induced ARDS model. ELISA results indicated that levels of serum IL-1β, IL-18, and TNFα were significantly increased in mice treated with LPS compared to those in control mice (Fig. 2A). Besides, the rate of apoptotic lung cells was significantly elevated in mice treated with LPS (Fig. 2B). Moreover, analysis of mouse lung tissues using H&E staining found that LPS dramatically induced lung injury by decreased pulmonary congestion and thinning the alveolar wall (Fig. 2C). Consistent with in vitro results, both NEAT1 silence and ACE2 overexpression by injection of lentivirus into mice abolished the effects of LPS in vivo (Fig. 2A-C). All these results suggest that NEAT1 enhances lung injury triggered by sepsis-induced ARDS via inhibiting ACE2 in vitro and in vivo.

NEAT1 declines the stability of *ACE2* mRNA through hnRNPA2B1 in sepsis-induced ARDS

The above results have shown that NEAT1 suppressed ACE2 expression. Therefore, we investigated the underlying mechanism of NEAT1 regulating ACE2 expression. As *ACE2* expression was reduced by NEAT1, a dual luciferase reporter assay was performed to determine whether NEAT1 regulated *ACE2* transcription. TSS and 2500 bp upstream TSS of human *ACE2* promoter were cloned into luciferase reporter gene plasmid pGL3 to construct reporter gene plasmid containing *ACE2* promoter (Supplementary Fig. S1). Nevertheless, co-transfection of NEAT1 siRNA did not affect the luciferase activity of AT-II cells transfected with reporter gene vectors containing *ACE2* promoter (Fig. 3A), suggesting that NEAT1 might influence ACE2 expression at the post-transcriptional level.

Next, the effect of NEAT1 on *ACE2* mRNA stability in AT-II cells was detected using RNA decay assays. Results showed that silence of NEAT1 by siRNA significantly increased the half-life ($t_{1/2}$) of *ACE2* mRNA (6.51 h) compared to that in the control group (3.52 h) (Fig. 3B). Additionally, siRNA NC did not affect the half-life of *ACE2* mRNA (3.46 h) (Fig. 3B), and actinomycin D treatment had no significant effect on GAPDH half-life ($t_{1/2}$) (Supplementary Fig. S2A). Thus, NEAT1 decreases ACE2 expression by reducing the stability of *ACE2* mRNA in AT-II cells.

To further elaborate on the mechanism of NEAT1 in regulating *ACE2* mRNA stability, RAP was carried out to identify RNAs and proteins associated with NEAT1 in AT-II cells. Results of RAP revealed that *ACE2* mRNA bound with NEAT1 (Fig. 3C). Besides, RNA binding protein hnRNPA2B1 also interacted with NEAT1 (Fig. 3D). Additionally, the RAP assay indicated that hnRNPA2B1 silence disrupted the association between NEAT1 and *ACE2* mRNA (Fig. 3E). Therefore, NEAT1 bound with

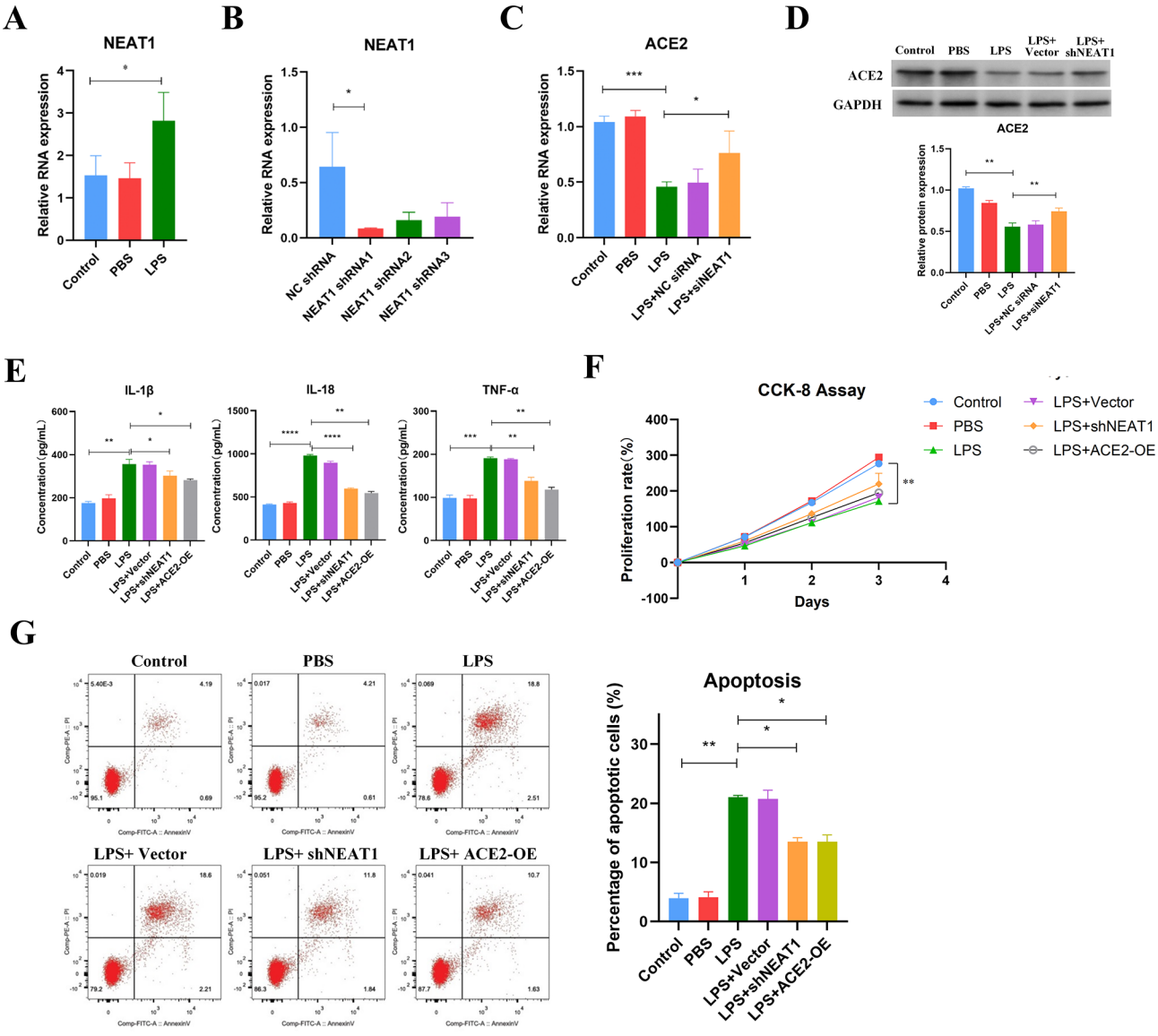

Fig. 1 NEAT1 aggravates lung injury caused by sepsis-induced ARDS through suppressing ACE2 in vitro. **A** The level of NEAT1 in AT-II cells, comparing those treated with or without LPS. **B** The level of NEAT1 in AT-II cells treated with or without shRNA. **C** The level of *ACE2* mRNA in AT-II cells transfected with or without NEAT1 siRNA under LPS condition. **D** The expression of ACE2 protein in AT-II cells transfected with or without NEAT1 siRNA under LPS condition. **E** The level of IL-1β, IL-18, and TNF-α in AT-II cells transfected with or without NEAT1 siRNA or ACE2 expression vector under LPS condition. **F** The proliferation rate of AT-II cells transfected with or without NEAT1 siRNA or ACE2 expression vector under LPS condition. **G** Representative images of flow cytometric apoptosis assay in AT-II cells transfected with or without NEAT1 siRNA or ACE2 expression vector under LPS condition. The bar graph shows the percentage of apoptotic cells in each group. Vector, blank pLP/VSVG vector; siNEAT1, NEAT1 siRNA; OE, overexpression. $N = 3$. $^{*}P < 0.05$, $^{**}P < 0.01$, $^{***}P < 0.001$, $^{****}P < 0.0001$. Quantitative data were presented as mean ± SD

ACE2 mRNA through hnRNPA2B1 in AT-II cells. Subsequently, the effect of hnRNPA2B1 on *ACE2* mRNA stability and expression in AT-II cells treated with LPS was determined. Results indicated that silence of hnRNPA2B1 by siRNA (Fig. 3F) improved the half-life ($t_{1/2}$) of *ACE2* mRNA (7.57 h) compared to that in the control group (3.34 h) (Fig. 3G) and upregulated *ACE2* mRNA expression under LPS condition (Fig. 3H). Additionally, actinomycin D treatment had no significant effect on GAPDH half-life ($t_{1/2}$) (Supplementary Fig. S2B). These results together suggest that NEAT1 reduces the stability of *ACE2* mRNA through hnRNPA2B1 in sepsis-induced ARDS.

RNA methylation contributes to NEAT1-dependent destabilization of *ACE2* mRNA in sepsis-induced ARDS

A recent study has demonstrated that m6A methylated lncRNA RP11 induces the mRNA degradation of E3 ligases through the formation of a methylated lncRNA RP11/hnRNPA2B1/ target mRNA complex [24].

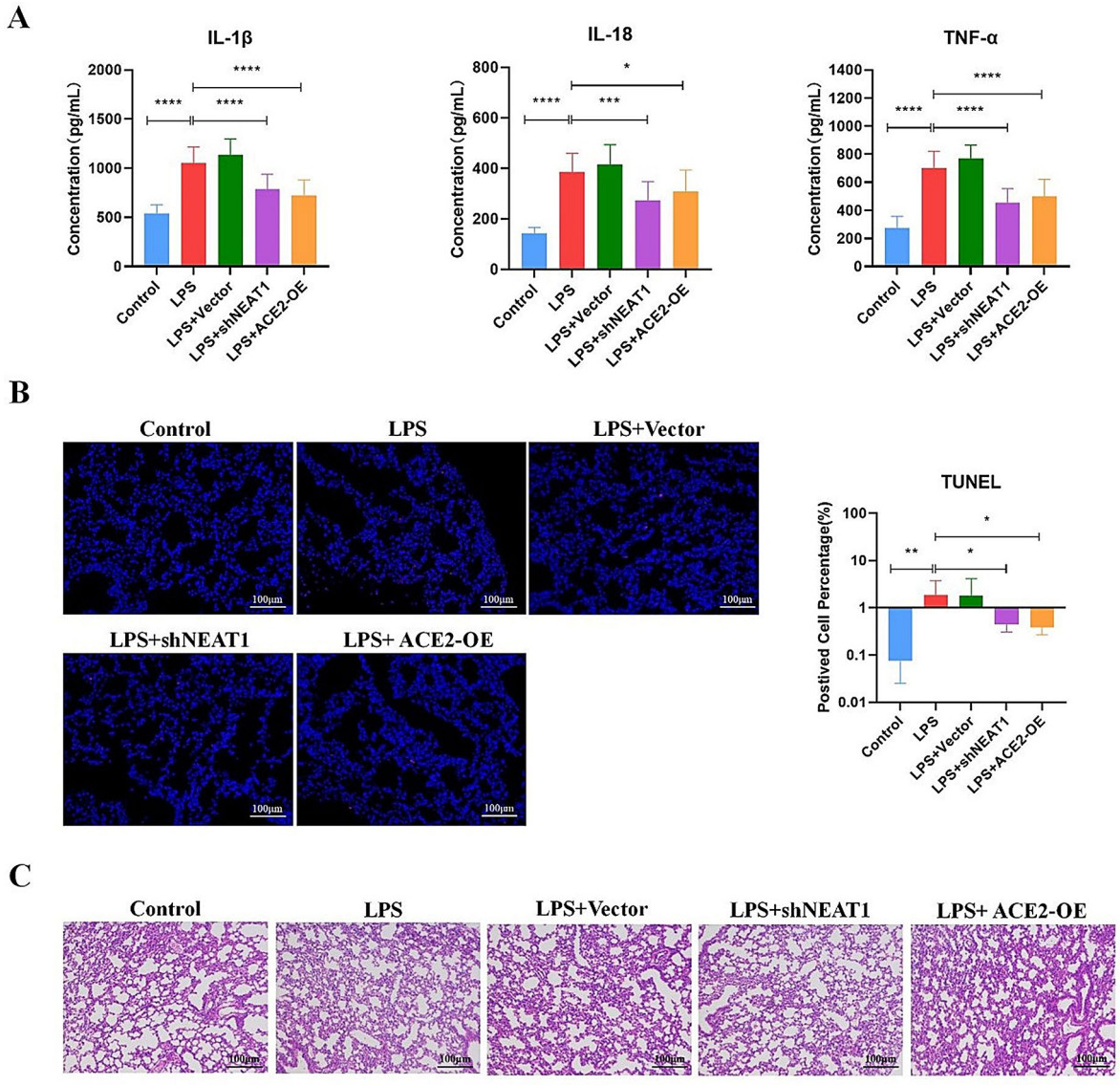

Fig. 2 NEAT1 aggravates lung injury caused by sepsis-induced ARDS through suppressing ACE2 in vivo. **A** The level of serum IL-1β, IL-18, and TNF-α in mice injected with or without shRNA-targeting NEAT1 or ACE2 expression vector under LPS condition. **B** Representative images of TUNEL assay in lung tissues of mice injected with or without shRNA-targeting NEAT1 or ACE2 expression vector under LPS condition. The bar graph shows the percentage of apoptotic cells in each group. Bars = 100 μm. **C** Representative images of mouse lung tissues with H&E staining. Bars = 100 μm. Vector, blank pLP/VSVG vector; shNEAT1, shRNA-targeting NEAT1; OE, overexpression. $N = 5$. $^{*}P < 0.05$, $^{**}P < 0.01$, $^{***}P < 0.001$, $^{****}P < 0.0001$. Quantitative data were presented as mean ± SD

Our results have shown that NEAT1 triggered *ACE2* mRNA degradation through hnRNPA2B1. However, whether RNA methylation was involved in this progress remains unknown. Thus, the role of RNA methylation in NEAT1-dependent destabilization of *ACE2* mRNA was investigated.

First, the methylation level of NEAT1 in AT-II cells was detected by Me-RIP. Results showed that LPS increased the m6A methylation level of NEAT1 in AT-II cells (Fig. 4A). Next, the silence of methyltransferase METTL3 and METTL14 by siRNAs (Fig. 4B) reduced the LPS-increased m6A methylation level of NEAT1 (Fig. 4A) but not *ACE2* mRNA (Supplementary Fig. S3) in AT-II cells. Furthermore, the half-life and level of *ACE2* mRNA were tested.

The half-life ($t_{1/2}$) of *ACE2* mRNA (8.84 h) was dramatically longer in METTL3 and METTL14-silenced AT-II cells than in control AT-II cells (3.87 h) under LPS condition (Fig. 4C). Besides, the silence of METTL3 and METTL14 increased *ACE2* mRNA levels in AT-II cells treated with LPS (Fig. 4D). Additionally, actinomycin D treatment had no significant effect on GAPDH half-life ($t_{1/2}$) (Supplementary Fig. S2C). These data suggest that NEAT1 destabilizes *ACE2* mRNA depending

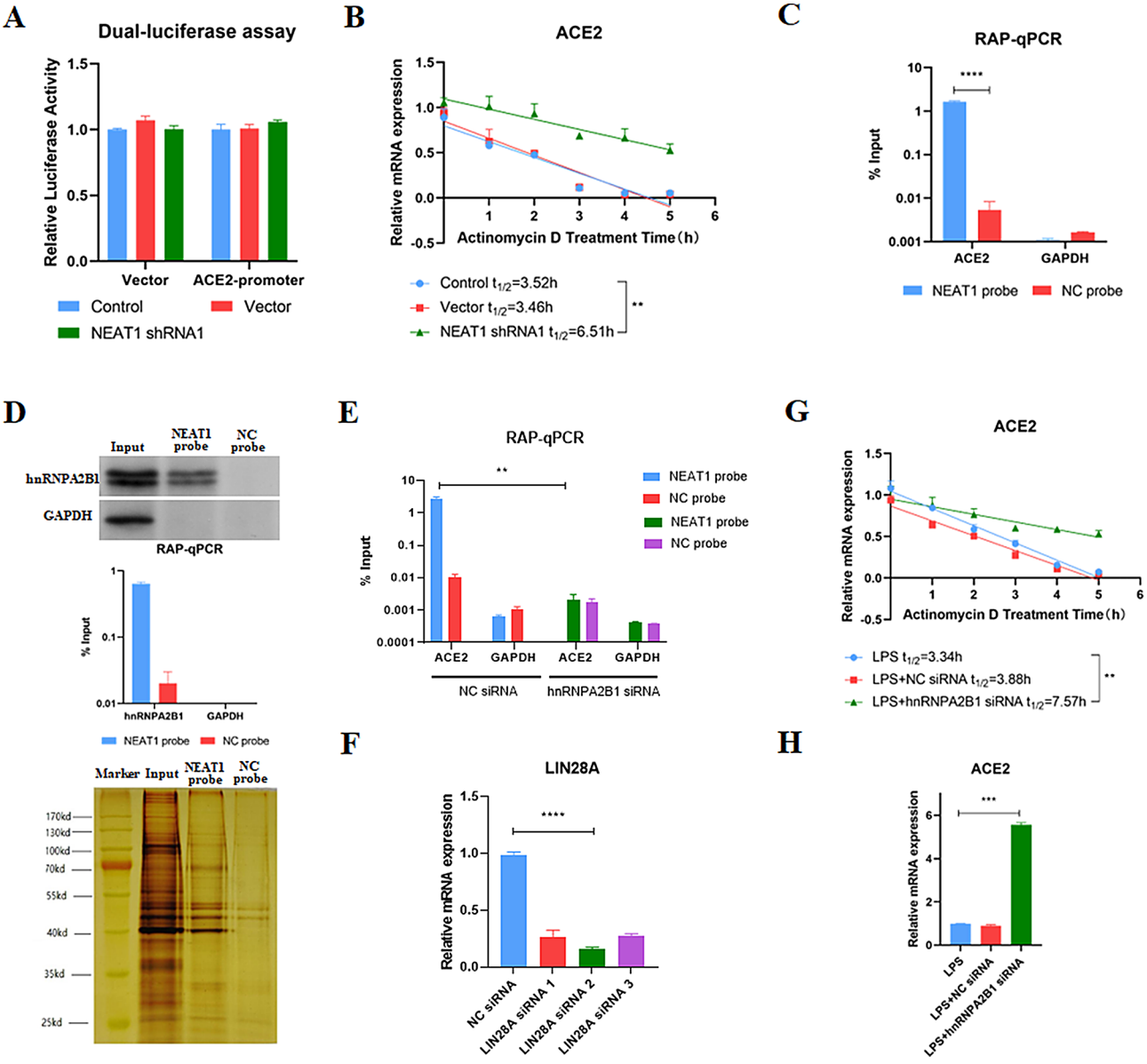

Fig. 3 NEAT1 declines the stability of *ACE2* mRNA through hnRNPA2B1 in sepsis-induced ARDS. **A** *ACE2* gene promoter activity analyzed by relative luciferase reporter activities in AT-II cells transfected with NEAT1 siRNA. **B** The level of *ACE2* mRNA in AT-II cells at 0 h, 1 h, 2 h, 3 h, 4 h, and 5 h after actinomycin D treatment identified by qRT-PCR. **C** Analysis of qRT-PCR for *ACE2* mRNA following RAP performed by probes-targeting NEAT1 in AT-II cells. **D** Representative images of WB for hnRNPA2B1 and silver staining following RAP performed by probes-targeting NEAT1 in AT-II cells. **E** Analysis of qRT-PCR for *ACE2* mRNA following RAP performed by probes-targeting NEAT1 in AT-II cells treated with or without hnRNPA2B1siRNA. **F** The level of hnRNPA2B1 mRNA in AT-II cells treated with or without siRNA. **G** The level of *ACE2* mRNA in AT-II cells treated with or without hnRNPA2B1 siRNA under LPS condition at 0 h, 1 h, 2 h, 3 h, 4 h, and 5 h after actinomycin D treatment identified by qRT-PCR. **H** The level of *ACE2* mRNA in AT-II cells treated with or without hnRNPA2B1 siRNA under LPS condition. Vector, blank pLP/VSVG vector. $N = 3$. $^{**}P < 0.01$, $^{***}P < 0.001$, $^{****}P < 0.0001$. Quantitative data were presented as mean ± SD

on RNA methylation by forming methylated NEAT1/hnRNPA2B1/*ACE2* mRNA complex in sepsis-induced ARDS.

LIN28A improves NEAT1 stability in sepsis-induced ARDS

Subsequently, the mechanism of LPS upregulating NEAT1 was elucidated. Results of RAP indicated that LIN28A protein was associated with NEAT1 in AT-II cells, and LPS enhanced the association between LIN28A protein and NEAT1 (Fig. 5A). It has been revealed that LIN28B, a homology of LIN28A, improves NEAT1 stability in ovarian cancer [30]. Thus, the effects of LIN28A in NEAT1 stability and expression were detected in AT-II cells.

Results showed that LIN28A silence by siRNA (Fig. 5B) decreased the half-life ($t_{1/2}$) of NEAT1 (3.21 h) compared to that in the control group (4.64 h) under LPS condition (Fig. 5C), similar to the effect of LIN28A silence on the

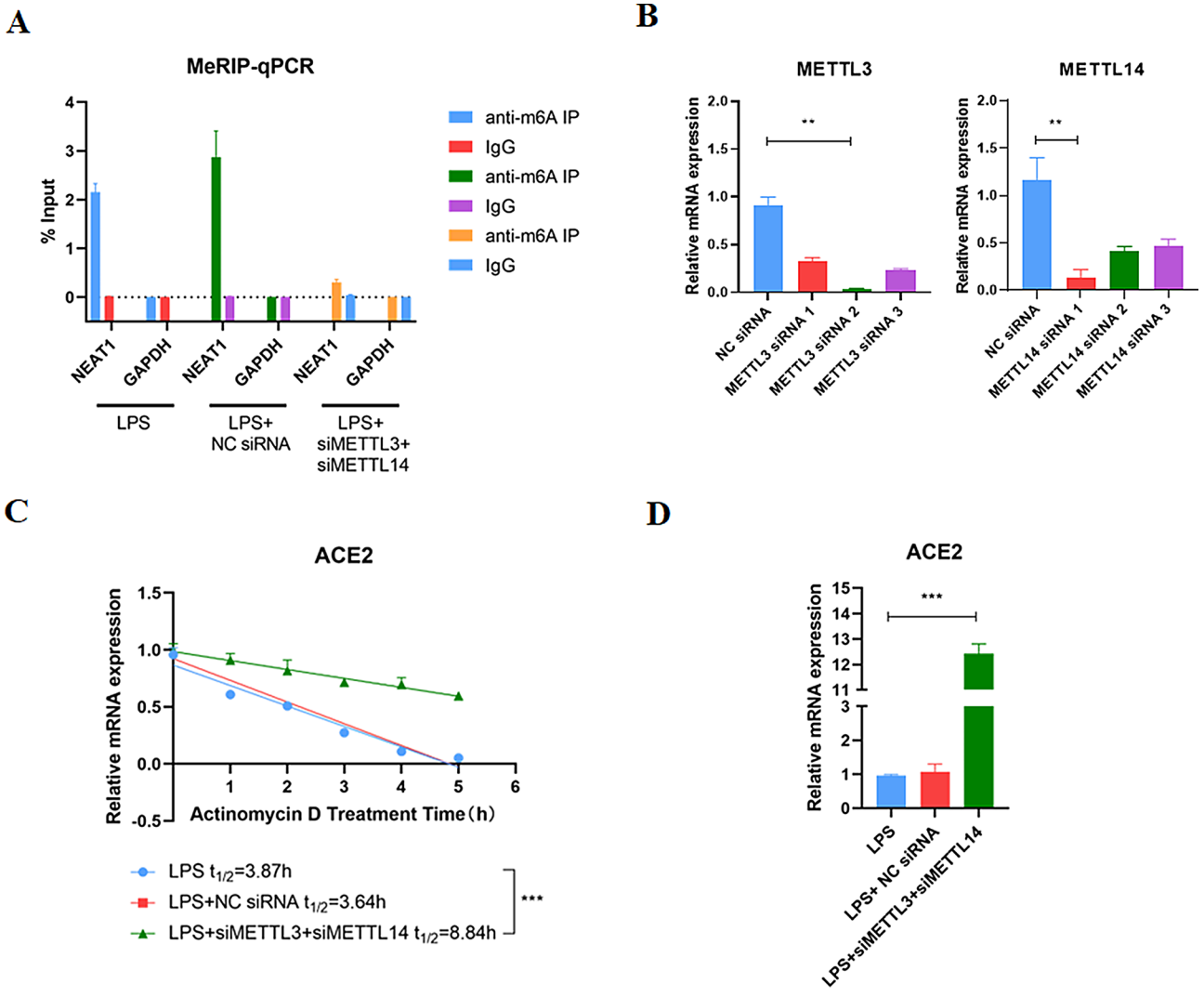

Fig. 4 RNA methylation contributes to NEAT1-dependent destabilization of *ACE2* mRNA in sepsis-induced ARDS. **A** The level of methylated NEAT1 in AT-II cells treated with or without METTL3 and METTL14 siRNAs under LPS condition detected by MeRIP. **B** The levels of METTL3 and METTL14 mRNA in AT-II cells treated with or without siRNAs. **C** The level of *ACE2* mRNA in AT-II cells treated with or without METTL3 and METTL14 siRNAs under LPS condition at 0 h, 1 h, 2 h, 3 h, 4 h, and 5 h after actinomycin D treatment identified by qRT-PCR. **D** The level of *ACE2* mRNA in AT-II cells treated with or without METTL3 and METTL14 siRNAs under LPS condition. NC, negative control; siMETTL3, METTL3 siRNA; siMETTL14, METTL14 siRNA. $N=3$. $^{**}P<0.01$, $^{***}P<0.001$. Quantitative data were presented as mean ± SD

stability of lncRNA metastasis associated lung adenocarcinoma transcript 1 (MALAT1) serving as a positive [31] (Supplementary Fig. S4 and S2D). Above data suggests that LIN28B improves NEAT1 stability in AT-II cells treated with LPS. Besides, siRNA NC did not affect the half-life of NEAT1 (4.10 h) (Fig. 5C), and actinomycin D treatment had no significant effect on GAPDH half-life ($t_{1/2}$) (Supplementary Fig. S2D). Moreover, the silence of LIN28A dramatically reduced NEAT1 level under LPS conditions (Fig. 5D). The above data suggest that LIN28A increases NEAT1 stability in sepsis-induced ARDS.

IGF2BP3 aggravates destabilization of NEAT1 by associating with LIN28A to disrupt the combination of LIN28A and NEAT1 in sepsis-induced ARDS

Results of RAP found that IGF2BP3 protein also interacted with NEAT1 (Fig. 6A). In contrast to LIN28A and LIN28B, IGF2BP3 can augment the destabilization of mRNA [32]. Indeed, RNA decay assays revealed that IGF2BP3 overexpression reduced the half-life ($t_{1/2}$) of NEAT1 (2.92 h) compared to that in the control group (4.07 h) under LPS condition (Fig. 6B), suggesting that IGF2BP3 exacerbates destabilization of NEAT1 in LPS-treated AT-II cells. Besides, actinomycin D treatment had no significant effect on GAPDH half-life ($t_{1/2}$) (Supplementary Fig. S2E). Moreover, IGF2BP3 overexpression

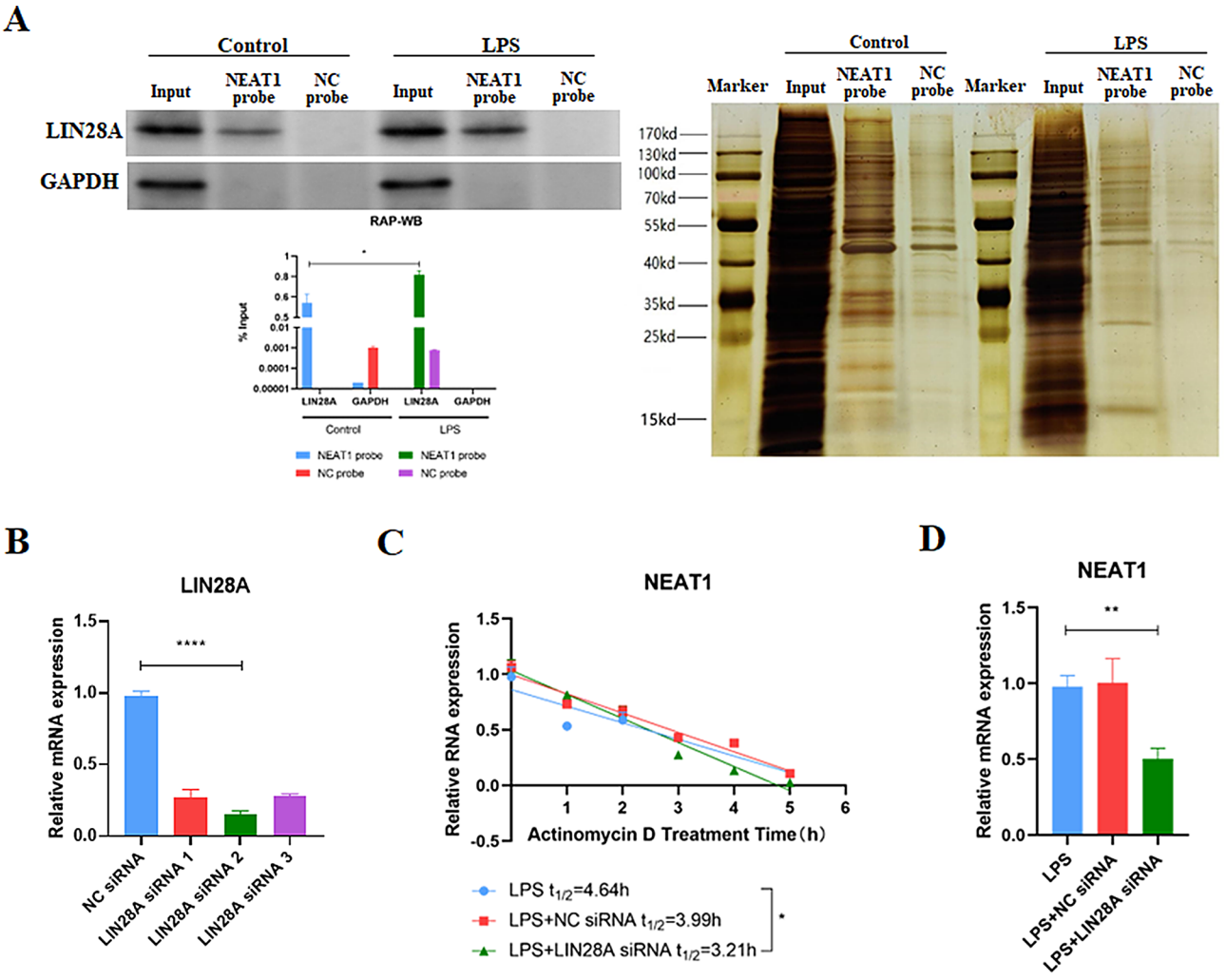

Fig. 5 LIN28A improves NEAT1 stability in sepsis-induced ARDS. **A** Representative images of WB for LIN28A and silver staining following RAP performed by probes-targeting NEAT1 in AT-II cells treated with or without LPS. **B** The level of LIN28A mRNA in AT-II cells treated with or without siRNA. **C** The level of *NEAT1* in AT-II cells treated with or without LIN28A siRNA under LPS condition at 0 h, 1 h, 2 h, 3 h, 4 h, and 5 h after actinomycin D treatment identified by qRT-PCR. **D** The level of *NEAT1* in AT-II cells treated with or without LIN28A siRNA under LPS condition. NC, negative control. $N = 3$. $^{*}P < 0.05$, $^{***}P < 0.001$, $^{****}P < 0.001$. Quantitative data were presented as mean ± SD

decreased NEAT1 levels under LPS conditions (Fig. 6C). Furthermore, results of Co-IP found that LIN28A bound with IGF2BP3 in AT-II cells, and LPS blocked the association between LIN28A and IGF2BP3 (Fig. 6D). Additionally, the results of RAP demonstrated that IGF2BP3 overexpression disrupted the interaction between LIN28A and NEAT1 in AT-II cells under LPS conditions, while blank expression vector did not affect the association between LIN28A and NEAT1 (Fig. 6E). All these data suggest that IGF2BP3 promotes destabilization of NEAT1 by associating with LIN28A to disrupt the combination of LIN28A and NEAT1 in sepsis-induced ARDS.

HnRNPA2B1 increases NEAT1 stability by blocking the interaction between LIN28A and IGF2BP3

The above data revealed that IGF2BP3 contributed to the destabilization of NEAT1 in sepsis-induced ARDS. However, the observed increase in NEAT1 level in sepsis-induced ARDS suggests the involvement of additional factors or regulatory mechanisms that counteract this destabilization. A previous study has uncovered that hnRNPA2B1 binds with IGF2BP3 [33]. Analysis by WB showed that LPS induced hnRNPA2B1 protein expression in AT-II cells (Fig. 7A). Besides, the results of Co-IP indicated that LPS facilitated the association between hnRNPA2B1 and IGF2BP3 in AT-II cells (Fig. 7B). Subsequently, results of Co-IP further determined that hnRNPA2B1 overexpression disrupted the interaction between IGF2BP3 and LIN28A under LPS conditions (Fig. 7C).

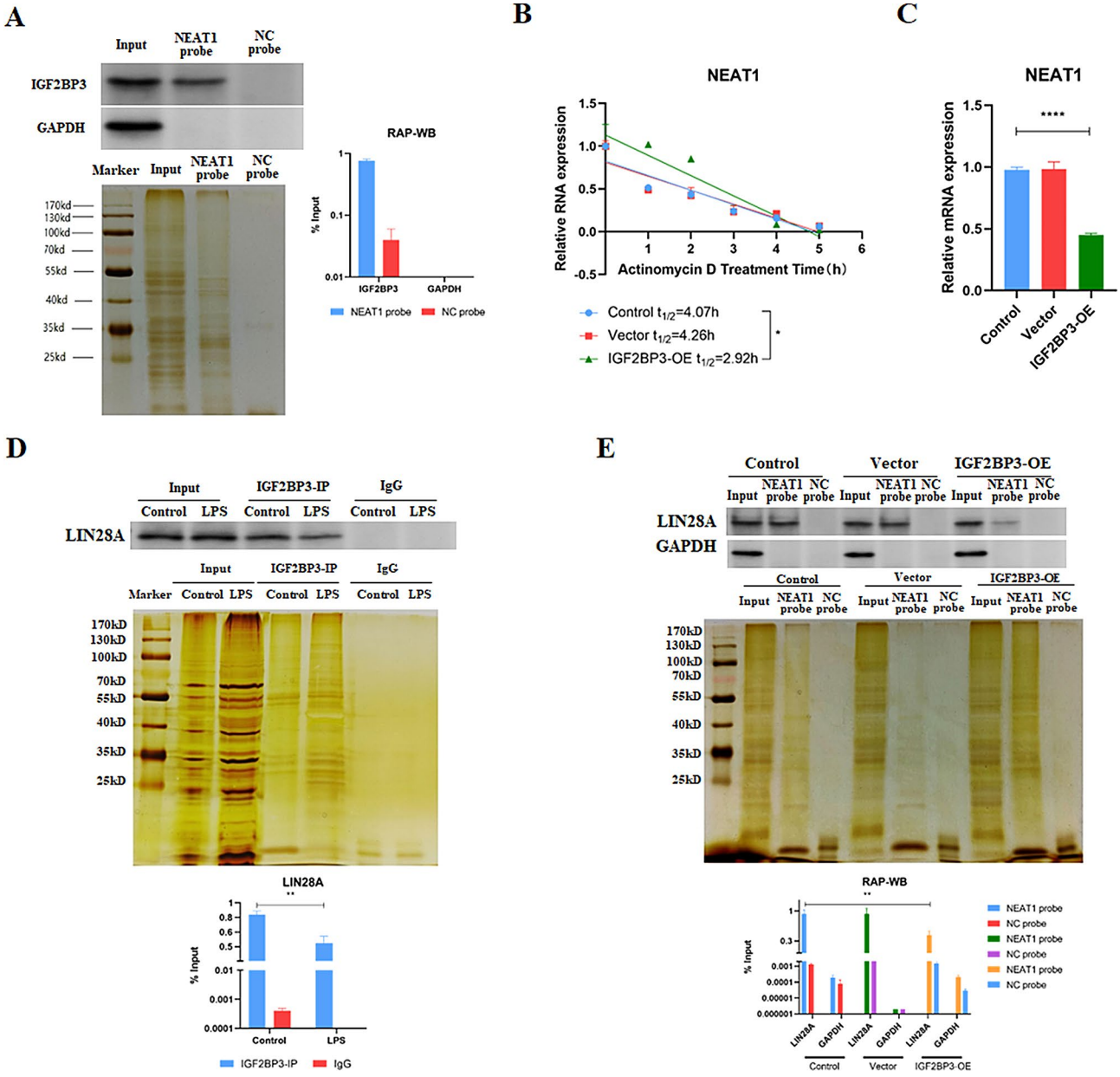

Fig. 6 IGF2BP3 aggravates destabilization of NEAT1 by associating with LIN28A to disrupt the combination of LIN28A and NEAT1 in sepsis-induced ARDS. **A** Representative images of WB for IGF2BP3 and silver staining following RAP performed by probes-targeting NEAT1 in AT-II cells. **B** The level of *NEAT1* in AT-II cells treated with or without IGF2BP3 expression vector at 0 h, 1 h, 2 h, 3 h, 4 h, and 5 h after actinomycin D treatment identified by qRT-PCR. **C** The level of *NEAT1* in AT-II cells treated with or without IGF2BP3 expression vector. **D** Representative images of WB for LIN28A and silver staining following Co-IP performed by IGF2BP3 antibody in AT-II cells treated with or without LPS. **E** Representative images of WB for LIN28A and silver staining following RAP performed by probes-targeting NEAT1 in AT-II cells treated with or without IGF2BP3 expression vector. NC, negative control; Vector, expression vector. $N = 3$. $^{*}P < 0.05$, $^{****}P < 0.0001$. Quantitative data were presented as mean ± SD

Thus, the effect of hnRNPA2B1 on NEAT1 stability was identified. Results found that silence of hnRNPA2B1 by siRNA decreased the half-life ($t_{1/2}$) of NEAT1 (3.27 h) compared to that in the control group (3.98 h) under LPS condition (Fig. 7D), suggesting that hnRNPA2B1 improves NEAT1 stability in LPS-treated AT-II cells. Besides, actinomycin D treatment had no significant effect on GAPDH half-life ($t_{1/2}$) (Supplementary Fig. S2B). Moreover, hnRNPA2B1 silence also reduced NEAT1 level under LPS conditions (Fig. 7E).

Therefore, our results reveal that NEAT1 reduces the stability of *ACE2* mRNA through hnRNPA2B1 depending on RNA methylation. Moreover, hnRNPA2B1 plays a dual role in both stabilizing NEAT1 and facilitating the degradation of *ACE2* mRNA.

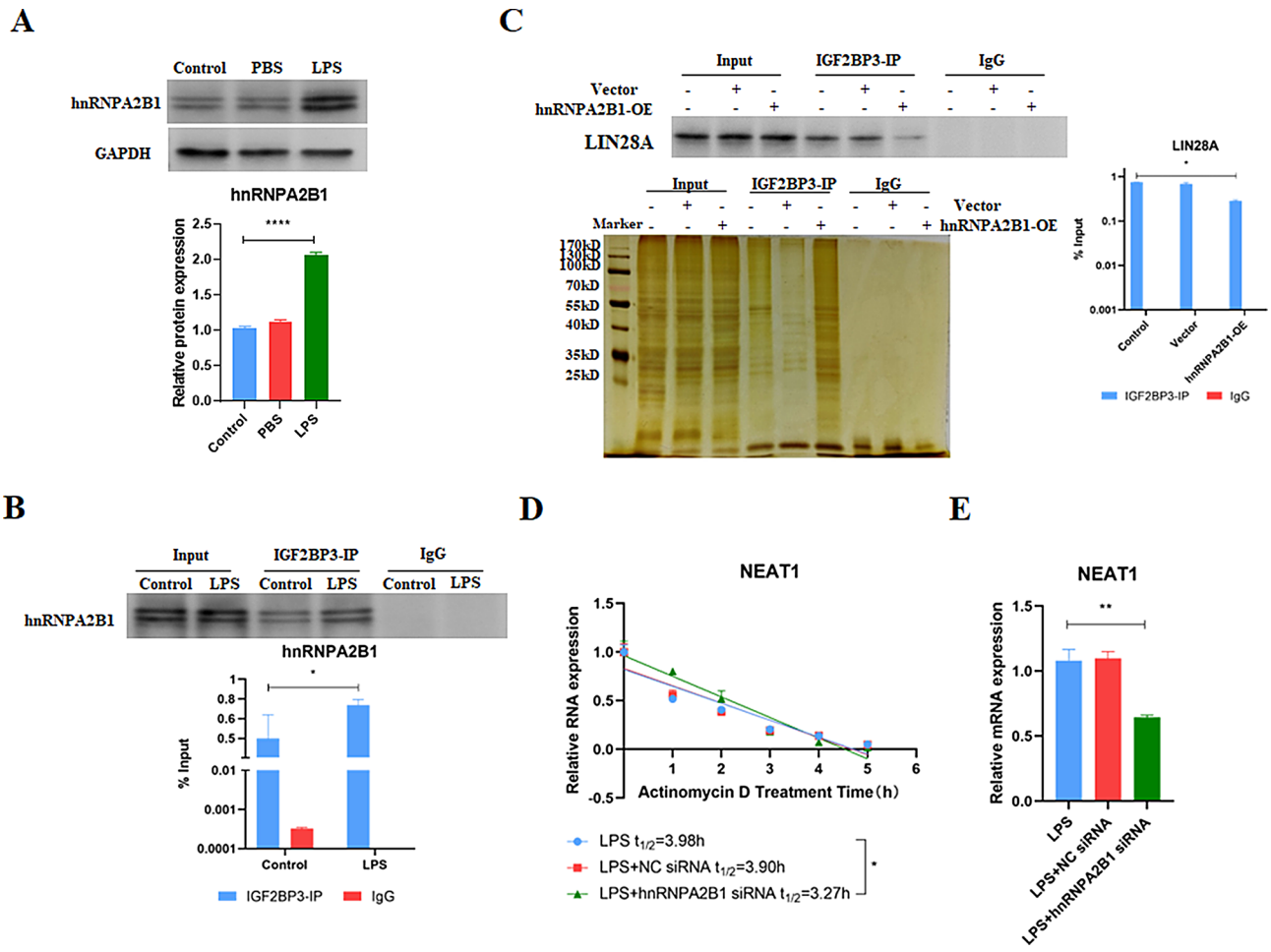

Fig. 7 HnRNPA2B1 increases NEAT1 stability by blocking the interaction between LIN28A and IGF2BP3. **A** The level of hnRNPA2B1 protein in AT-II cells treated with or without LPS. **B** Representative images of WB for hnRNPA2B1 and silver staining following Co-IP performed by IGF2BP3 antibody in AT-II cells treated with or without LPS. As samples were identical with those used for Fig. 6D, the representative image of silver staining following Co-IP was present in Fig. 6D. **C** Representative images of WB for LIN28A and silver staining following Co-IP performed by IGF2BP3 antibody in AT-II cells treated with or without hnRNPA2B1 expression vector. **D** The level of *NEAT1* in AT-II cells treated with or without hnRNPA2B1 siRNA under LPS condition at 0 h, 1 h, 2 h, 3 h, 4 h, and 5 h after actinomycin D treatment identified by qRT-PCR. **E** The level of NEAT1 in AT-II cells treated with or without hnRNPA2B1 siRNA under LPS condition. OE, overexpression. $N = 3$. $^{*}P < 0.05$, $^{**}P < 0.01$. Quantitative data were presented as mean ± SD

Discussion

This study suggests that NEAT1 aggravates lung injury by suppressing ACE2 in sepsis-induced ARDS models in vitro and in vivo. Mechanistically, NEAT1 decreased the stability of *ACE2* mRNA through hnRNPA2B1 in LPS-treated AT-II cells. Furthermore, NEAT1 destabilized *ACE2* mRNA through RNA methylation by forming a methylated NEAT1/hnRNPA2B1/*ACE2* mRNA complex in AT-II cells under LPS conditions. Additionally, LIN28A enhanced NEAT1 stability whereas IGF2BP3 promoted NEAT1destabilization by associating with LIN28A to disrupt the LIN28A and NEAT1 complex in LPS-treated AT-II cells. However, hnRNPA2B1 increased NEAT1 stability by blocking the interaction between LIN28A and IGF2BP3 in AT-II cells under LPS conditions.

This study demonstrates an increase in NEAT1 methylation level in AT-II cells under LPS conditions. However, the potential mechanism of LPS increasing NEAT1 methylation level was not investigated in the present study. A recent study has found that LPS treatment reduces the expression of a m6A eraser protein fat mass and obesity-associated protein (FTO) to increase m6A methylation in the myocardium of mice [34]. Therefore, it is plausible that LPS administration might increase NEAT1 methylation level by decreasing FTO expression in AT-II cells.

Our results reveal, for the first time, the inhibitory effects of NEAT1 on ACE2 expression in sepsis-induced ARDS. To date, the effects of lncRNAs on ACE2 remain unclear. Only one study has revealed that lncRNA ALT1 regulates the cell cycle through activating ACE2 in vascular endothelial cells [35]. Consequently, our findings significantly contribute to expanding the current knowledge

about the intricate roles of lncRNAs, particularly in the modulation of ACE2.

Our results indicates that NEAT1 has no effect on *ACE2* transcription by dual-luciferase reporter assay. However, lncRNA could modify chromatin dynamics to regulate gene transcription [36], which could not be elucidated via dual-luciferase reporter assay. Therefore, it is necessary to further verify whether NEAT1 regulated *ACE2* transcription by modulating chromatin dynamics in AT-II cells.

Several studies have shed light on the role of NEAT1 in mRNA stability. For instance, NEAT1 interacts with E74 like ETS transcription factor 3 (ELF3) mRNA to suppress *ELF3* mRNA degradation by facilitating the association between IGF2BP1 protein and *ELF3* mRNA [37]. Besides, NEAT1 protects mouse neurons against ischemia stroke-induced injury through binding with wingless-type MMTV integration site family, member 3 A (Wnt3a) mRNA to improve its stability via U2 small nuclear RNA auxiliary factor 2 (U2AF2) [38]. However, the role of RNA methylation in NEAT1-dependent destabilization of mRNA remains unexplored in current literature. Thus, the present study revealed that RNA methylation contributed to NEAT1-dependent destabilization of mRNA for the first time.

The present study elucidates, for the first time, the role of RNA methylation in NEAT1-dependent mRNA destabilization. NEAT1 destabilized *ACE2* mRNA depending on RNA methylation by forming methylated NEAT1/hnRNPA2B1/*ACE2* mRNA complex. It has been reported that hnRNPA2B1 induces mRNA decay by forming complexes with lncRNAs. For example, hnRNPA2B1 associates with lncRNA lncHC to induce degradation of cytochrome P450 family 7 subfamily A member 1 (Cyp7a1) and ATP binding cassette subfamily A member 1 (Abca1) mRNAs after binding to these two mRNAs in hepatocytes [39]. Besides, lncRNA miR503HG interacts with *p52* and *p65* mRNA to reduce their stability by hnRNPA2B1 [40]. Nevertheless, the role of RNA methylation in hnRNPA2B1/lncRNA complex-mediated mRNA destabilization is not clear. So far, only one study has demonstrated that lncRNARP11 triggers the mRNA degradation of E3 ligases by methylated lncRNA RP11/hnRNPA2B1/mRNA complex [24]. This finding suggests that RNA methylation might represent a novel avenue for exploration in understanding hnRNPA2B1/lncRNA complex-mediated mRNA destabilization. Numerous RNA-binding proteins have been identified as regulators of NEAT1 stability. A previous study has found that HuR increases NEAT1 stability to promote ovarian carcinogenesis [41]. Besides, a recent study has reported that the AUF1 protein enhances NEAT1 stability via adenosine deaminase acting on RNA-1 (ADAR1) in atherosclerotic cardiovascular disease [42]. Moreover, the RNA demethylase alkB homolog 5 (ALKBH5) improves NEAT1 stability by erasing m6A deposition from NEAT1 in glioblastoma multiforme [43]. By contrast, arsenic resistance protein 2 (ARS2) reduces NEAT1 stability to inhibit the formation of paraspeckles [44]. However, the effects of LIN28A, IGF2BP3, and hnRNPA2B1 on NEAT1 stability are largely unknown. Thus, our results indicate the promotive roles of LIN28A and hnRNPA2B1 and the suppressive role of IGF2BP3 in NEAT1 stability for the first time.

Although the effects of LIN28A and IGF2BP3 on NEAT1 stability remain unclear, the regulator effects of LIN28A and IGF2BP3 on other lncRNAs have been reported. For instance, LIN28A could stabilize lncRNA small nucleolar RNA host gene 14 (SNHG14) to facilitate aerobic glycolysis in glioma [45]. Besides, LIN28A stabilizes lncRNA FBXL19 antisense RNA 1 (FBXL19-AS1) in breast cancer to trigger metastasis [46].

In addition, IGF2BP3 has been reported to enhance the stability of lncRNA cyclin-dependent kinase inhibitor 2B antisense RNA 1 (CDKN2B-AS1) in renal clear cell carcinoma and promote disease progression [47]. Moreover, IGF2BP3 stabilizes methylated lncRNA KCNMB2 antisense RNA 1 (KCNMB2-AS1) to enhance cell growth in cervical cancer [48]. Nevertheless, the role of hnRNPA2B1 in lncRNA stability is unknown. Overall, the current study uncovers the role of hnRNPA2B1 in lncRNA stability for the first time. Meanwhile, our findings reveals the suppressive role of IGF2BP3 in lncRNA stability by contrast to those in previous studies.

Nevertheless, certain limitations should be acknowledged in the present study. For instance, a cecal ligation and puncture (CLP) experimental sepsis animal model is better than the LPS experimental sepsis animal model. Besides, the current study could be strengthened by determining the mechanism of LPS increasing NEAT1 methylation level. Moreover, it is necessary to further verify whether NEAT1 regulated *ACE2* transcription by modulating chromatin dynamics in AT-II cells. Moreover, the findings of this study should be confirmed via in vivo experiments.

Conclusion

This study indicates that NEAT1 aggravates lung injury through destabilizing *ACE2* mRNA by forming methylated NEAT1/hnRNPA2B1/*ACE2* mRNA complex in sepsis-induced ARDS. Additionally, hnRNPA2B1 enhances LIN28A-mediated NEAT1 stability by disrupting the interaction between LIN28A and IGF2BP3 in sepsis-induced ARDS (Fig. 8). These findings not only shed light on the intricate mechanism underlying sepsis-induced ARDS but also unveil promising therapeutic targets for this condition.

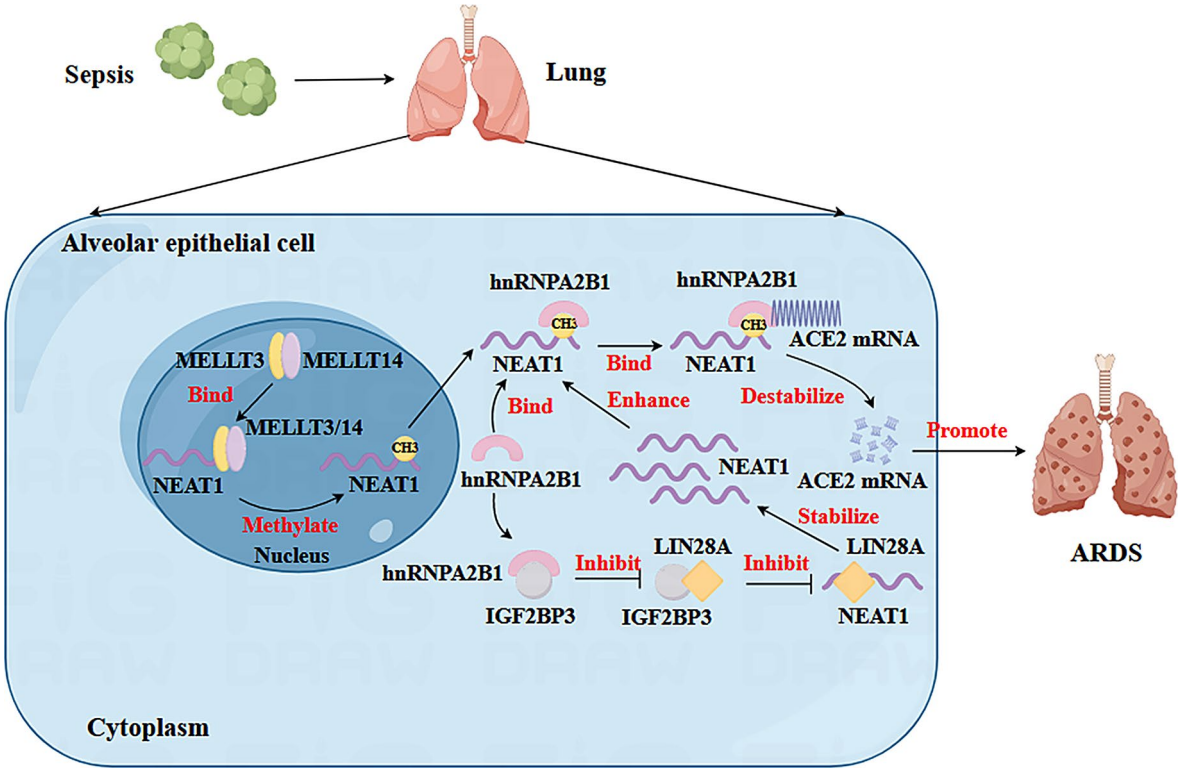

Fig. 8 Schematic diagram of molecular mechanisms for the present study. NEAT1 aggravated lung injury through suppressing ACE2 through destabilizing *ACE2* mRNA depending on RNA methylation by forming methylated NEAT1/hnRNPA2B1/*ACE2* mRNA complex in sepsis-induced ARDS model. Moreover, hnRNPA2B1 improved LIN28A-mediated NEAT1 stability by blocking the interaction between LIN28A and IGF2BP3 in the sepsis-induced ARDS model

Supplementary Information

The online version contains supplementary material available at https://doi.org/10.1186/s12967-024-06032-7.

Supplementary Material 1

Acknowledgements
Not applicable.

Author contributions
JL, XL, PY, ZY, and YF contributed to the study conception and design. Material preparation and experiments were performed by JL, XL, PY, YH, and WH. Data collection and analysis were performed by JL, XL, PY, ZY, and YF. The manuscript was written by JL, XL, PY, ZY and YF. All authors read and approved the final manuscript.

Funding
Not applicable.

Data availability
The datasets used and analyzed during the current study are available from the corresponding author upon reasonable request.

Declarations

Ethics approval and consent to participate
All animal experiments were approved by the Animal Ethics Committee of Sun Yat-sen University (#SYSU-IACUC-2022-000058).

Consent for publication
Not applicable.

Competing interests
The authors declare that they have no competing interests.

Author details
[1]Department of Anesthesiology, The Third Affiliated Hospital, Sun Yat-Sen University, Guangzhou 510630, China
[2]Department of Anesthesiology, The First Affiliated Hospital, Sun Yat-Sen University, Guangzhou 510080, China
[3]Intensive Care Unit, The Third Affiliated Hospital, Sun Yat-Sen University, Guangzhou 510630, China
[4]Emergency Department, The Third Affiliated Hospital, Sun Yat-Sen University, Guangzhou 510630, China

Received: 24 July 2024 / Accepted: 25 December 2024
Published online: 06 January 2025

References

1. Thompson BT, Chambers RC, Liu KD. Acute respiratory distress syndrome. N Engl J Med. 2017;377:562–72.
2. Nanchal RS, Truwit JD. Recent advances in understanding and treating acute respiratory distress syndrome. F1000Res. 2018;7.
3. Meyer NJ, Gattinoni L, Calfee CS. Acute respiratory distress syndrome. Lancet. 2021;398:622–37.
4. Kaku S, Nguyen CD, Htet NN, Tutera D, Barr J, Paintal HS, Kuschner WG. Acute respiratory distress syndrome: etiology, Pathogenesis, and Summary on Management. J Intensive Care Med. 2020;35:723–37.
5. Bellani G, Laffey JG, Pham T, Fan E, Brochard L, Esteban A, Gattinoni L, van Haren F, Larsson A, McAuley DF, et al. Epidemiology, patterns of Care, and mortality for patients with Acute Respiratory Distress Syndrome in Intensive Care Units in 50 countries. JAMA. 2016;315:788–800.

6. Fan E, Beitler JR, Brochard L, Calfee CS, Ferguson ND, Slutsky AS, Brodie D. COVID-19-associated acute respiratory distress syndrome: is a different approach to management warranted? Lancet Respir Med. 2020;8:816–21.
7. De Freitas Caires N, Gaudet A, Portier L, Tsicopoulos A, Mathieu D, Lassalle P. Endocan, sepsis, pneumonia, and acute respiratory distress syndrome. Crit Care. 2018;22:280.
8. Cohen J, Vincent JL, Adhikari NK, Machado FR, Angus DC, Calandra T, Jaton K, Giulieri S, Delaloye J, Opal S, et al. Sepsis: a roadmap for future research. Lancet Infect Dis. 2015;15:581–614.
9. Hu Q, Hao C, Tang S. From sepsis to acute respiratory distress syndrome (ARDS): emerging preventive strategies based on molecular and genetic researches. Biosci Rep. 2020;40.
10. Kerchberger VE, Bastarache JA, Shaver CM, Nagata H, McNeil JB, Landstreet SR, Putz ND, Yu WK, Jesse J, Wickersham NE et al. Haptoglobin-2 variant increases susceptibility to acute respiratory distress syndrome during sepsis. JCI Insight. 2019;4.
11. Ling Y, Li ZZ, Zhang JF, Zheng XW, Lei ZQ, Chen RY, Feng JH. MicroRNA-494 inhibition alleviates acute lung injury through Nrf2 signaling pathway via NQO1 in sepsis-associated acute respiratory distress syndrome. Life Sci. 2018;210:1–8.
12. Yamaguchi T, Hoshizaki M, Minato T, Nirasawa S, Asaka MN, Niiyama M, Imai M, Uda A, Chan JF, Takahashi S, et al. ACE2-like carboxypeptidase B38-CAP protects from SARS-CoV-2-induced lung injury. Nat Commun. 2021;12:6791.
13. Hoffmann M, Kleine-Weber H, Schroeder S, Kruger N, Herrler T, Erichsen S, Schiergens TS, Herrler G, Wu NH, Nitsche A, et al. SARS-CoV-2 cell entry depends on ACE2 and TMPRSS2 and is blocked by a clinically proven protease inhibitor. Cell. 2020;181:271–e280278.
14. Imai Y, Kuba K, Rao S, Huan Y, Guo F, Guan B, Yang P, Sarao R, Wada T, Leong-Poi H, et al. Angiotensin-converting enzyme 2 protects from severe acute lung failure. Nature. 2005;436:112–6.
15. Kuba K, Imai Y, Rao S, Gao H, Guo F, Guan B, Huan Y, Yang P, Zhang Y, Deng W, et al. A crucial role of angiotensin converting enzyme 2 (ACE2) in SARS coronavirus-induced lung injury. Nat Med. 2005;11:875–9.
16. Meydan C, Madrer N, Soreq H. The Neat Dance of COVID-19: NEAT1, DANCR, and co-modulated cholinergic RNAs link to inflammation. Front Immunol. 2020;11:590870.
17. Yang Y, Yang L, Liu Z, Wang Y, Yang J. Long noncoding RNA NEAT 1 and its target microRNA-125a in sepsis: correlation with acute respiratory distress syndrome risk, biochemical indexes, disease severity, and 28-day mortality. J Clin Lab Anal. 2020;34:e23509.
18. Lv X, Zhang XY, Zhang Q, Nie YJ, Luo GH, Fan X, Yang S, Zhao QH, Li JQ. lncRNA NEAT1 aggravates sepsis-induced lung injury by regulating the miR-27a/PTEN axis. Lab Invest. 2021;101:1371–81.
19. Zhou H, Wang X, Zhang B. Depression of lncRNA NEAT1 Antagonizes LPS-Evoked Acute Injury and Inflammatory Response in Alveolar Epithelial Cells via HMGB1-RAGE Signaling. Mediators Inflamm. 2020;2020:8019467.
20. Pan Y, Ma P, Liu Y, Li W, Shu Y. Multiple functions of m(6)a RNA methylation in cancer. J Hematol Oncol. 2018;11:48.
21. Du J, Liao W, Liu W, Deb DK, He L, Hsu PJ, Nguyen T, Zhang L, Bissonnette M, He C, Li YC. N(6)-Adenosine methylation of Socs1 mRNA is required to sustain the negative feedback control of macrophage activation. Dev Cell. 2020;55:737–e753737.
22. Wang H, Wang Q, Chen J, Chen C. Association among the gut Microbiome, the serum Metabolomic Profile and RNA m(6)a methylation in Sepsis-Associated Encephalopathy. Front Genet. 2022;13:859727.
23. Jia Y, Yan Q, Zheng Y, Li L, Zhang B, Chang Z, Wang Z, Tang H, Qin Y, Guan XY. Long non-coding RNA NEAT1 mediated RPRD1B stability facilitates fatty acid metabolism and lymph node metastasis via c-Jun/c-Fos/SREBP1 axis in gastric cancer. J Exp Clin Cancer Res. 2022;41:287.
24. Wu Y, Yang X, Chen Z, Tian L, Jiang G, Chen F, Li J, An P, Lu L, Luo N, et al. M(6) A-induced lncRNA RP11 triggers the dissemination of colorectal cancer cells via upregulation of Zeb1. Mol Cancer. 2019;18:87.
25. Ning QM, Wang XR. Response of alveolar type II epithelial cells to mechanical stretch and lipopolysaccharide. Respiration. 2007;74:579–85.
26. Ning QM, Sun XN, Zhao XK. Role of mechanical stretching and lipopolysaccharide in early apoptosis and IL-8 of alveolar epithelial type II cells A549. Asian Pac J Trop Med. 2012;5:638–44.
27. Sun L, Zhang Y, Huang CX, Qu XL, Zhang Y, Zhang JC, Wei X, Zhuang Y, Zhai S, Peng MJ, et al. Therapeutic effect of RANTES-KDEL on inhibition of HIV-1 in CD34(+) human hematopoietic stem cells (hHSC). J Virol Methods. 2008;154:194–9.
28. Zhang Y, Xu X, Ceylan-Isik AF, Dong M, Pei Z, Li Y, Ren J. Ablation of Akt2 protects against lipopolysaccharide-induced cardiac dysfunction: role of akt ubiquitination E3 ligase TRAF6. J Mol Cell Cardiol. 2014;74:76–87.
29. Ren J, Xu X, Wang Q, Ren SY, Dong M, Zhang Y. Permissive role of AMPK and autophagy in adiponectin deficiency-accentuated myocardial injury and inflammation in endotoxemia. J Mol Cell Cardiol. 2016;93:18–31.
30. Yong W, Yu D, Jun Z, Yachen D, Weiwei W, Midie X, Xingzhu J, Xiaohua W. Long noncoding RNA NEAT1, regulated by LIN28B, promotes cell proliferation and migration through sponging miR-506 in high-grade serous ovarian cancer. Cell Death Dis. 2018;9:861.
31. Wang Z, Pang J, Ji B, Zhang S, Cheng Y, Yu L, Pan W. RNA binding protein Lin28A promotes osteocarcinoma cells progression by associating with the long noncoding RNA MALAT1. Biotechnol Lett. 2018;40:493–500.
32. Mizutani R, Imamachi N, Suzuki Y, Yoshida H, Tochigi N, Oonishi T, Suzuki Y, Akimitsu N. Oncofetal protein IGF2BP3 facilitates the activity of proto-oncogene protein eIF4E through the destabilization of EIF4E-BP2 mRNA. Oncogene. 2016;35:3495–502.
33. Kristensen AR, Gsponer J, Foster LJ. A high-throughput approach for measuring temporal changes in the interactome. Nat Methods. 2012;9:907–9.
34. Dubey PK, Patil M, Singh S, Dubey S, Ahuja P, Verma SK, Krishnamurthy P. Increased m6A-RNA methylation and FTO suppression is associated with myocardial inflammation and dysfunction during endotoxemia in mice. Mol Cell Biochem. 2022;477:129–41.
35. Li W, Wang R, Ma JY, Wang M, Cui J, Wu WB, Liu RM, Zhang CX, Li W, Wang SM. A human long non-coding RNA ALT1 controls the cell cycle of vascular endothelial cells Via ACE2 and Cyclin D1 pathway. Cell Physiol Biochem. 2017;43:1152–67.
36. Bhan A, Mandal SS. LncRNA HOTAIR: a master regulator of chromatin dynamics and cancer. Biochim Biophys Acta. 2015;1856:151–64.
37. Feng Y, Gao L, Cui G, Cao Y. LncRNA NEAT1 facilitates pancreatic cancer growth and metastasis through stabilizing ELF3 mRNA. Am J Cancer Res. 2020;10:237–48.
38. Zhou Z, Ren X, Zheng L, Li A, Zhou W. LncRNA NEAT1 stabilized Wnt3a via U2AF2 and activated Wnt/beta-catenin pathway to alleviate ischemia stroke induced injury. Brain Res. 2022;1788:147921.
39. Lan X, Yan J, Ren J, Zhong B, Li J, Li Y, Liu L, Yi J, Sun Q, Yang X, et al. A novel long noncoding RNA Lnc-HC binds hnRNPA2B1 to regulate expressions of Cyp7a1 and Abca1 in hepatocytic cholesterol metabolism. Hepatology. 2016;64:58–72.
40. Wang H, Liang L, Dong Q, Huan L, He J, Li B, Yang C, Jin H, Wei L, Yu C, et al. Long noncoding RNA miR503HG, a prognostic indicator, inhibits tumor metastasis by regulating the HNRNPA2B1/NF-kappaB pathway in hepatocellular carcinoma. Theranostics. 2018;8:2814–29.
41. Chai Y, Liu J, Zhang Z, Liu L. HuR-regulated lncRNA NEAT1 stability in tumorigenesis and progression of ovarian cancer. Cancer Med. 2016;5:1588–98.
42. Vlachogiannis NI, Sachse M, Georgiopoulos G, Zormpas E, Bampatsias D, Delialis D, Bonini F, Galyfos G, Sigala F, Stamatelopoulos K, et al. Adenosine-to-inosine Alu RNA editing controls the stability of the pro-inflammatory long noncoding RNA NEAT1 in atherosclerotic cardiovascular disease. J Mol Cell Cardiol. 2021;160:111–20.
43. Dong F, Qin X, Wang B, Li Q, Hu J, Cheng X, Guo D, Cheng F, Fang C, Tan Y, et al. ALKBH5 facilitates Hypoxia-Induced Paraspeckle Assembly and IL8 Secretion to generate an immunosuppressive Tumor Microenvironment. Cancer Res. 2021;81:5876–88.
44. Machitani M, Taniguchi I, Ohno M. ARS2 Regulates Nuclear Paraspeckle Formation through 3'-End Processing and Stability of NEAT1 Long Noncoding RNA. Mol Cell Biol. 2020;40.
45. Lu J, Liu X, Zheng J, Song J, Liu Y, Ruan X, Shen S, Shao L, Yang C, Wang D, et al. Lin28A promotes IRF6-regulated aerobic glycolysis in glioma cells by stabilizing SNHG14. Cell Death Dis. 2020;11:447.
46. Zhang Y, Xiao X, Zhou W, Hu J, Zhou D. LIN28A-stabilized FBXL19-AS1 promotes breast cancer migration, invasion and EMT by regulating WDR66. Vitro Cell Dev Biol Anim. 2019;55:426–35.
47. Xie X, Lin J, Fan X, Zhong Y, Chen Y, Liu K, Ren Y, Chen X, Lai D, Li X, et al. LncRNA CDKN2B-AS1 stabilized by IGF2BP3 drives the malignancy of renal clear cell carcinoma through epigenetically activating NUF2 transcription. Cell Death Dis. 2021;12:201.

48. Zhang Y, Wang D, Wu D, Zhang D, Sun M. Long noncoding RNA KCNMB2-AS1 stabilized by N(6)-Methyladenosine modification promotes cervical Cancer Growth through acting as a competing endogenous RNA. Cell Transpl. 2020;29:963689720964382.

Publisher's note